Research Square

Preprints are preliminary reports that have not undergone peer review.
They should not be considered conclusive, used to inform clinical practice,
or referenced by the media as validated information.

The Neglected Canal: A Study on the Canal Incidence and Anatomical Characteristics of the Posterior Molar Canal

Bolun Zhang
Xi'an Medical University
Siyu He
Xi'an Medical University
Yuan Li
Guizhou Provincial People's Hospital
Zhuolin Han
Xi'an Medical University
Lihao Zhang
Su Liu
Xingxing Mu
Fei Liang
liangfei662003@foxmail.com
Xi'an Medical University
Kaijin Hu
Xi'an Medical University

Research Article

Keywords: Posterior molar canal, Retromolar canal, Cone-beam computed tomography, Magnetic resonance imaging, Mandibular third molar, Anatomical variation

Posted Date: July 27th, 2026

DOI: https://doi.org/10.21203/rs.3.rs-10408894/v1

License: This work is licensed under a Creative Commons Attribution 4.0 International License.
Read Full License

Additional Declarations: No competing interests reported.

Abstract

Background

The posterior molar canal (PMC) has been implicated as a potential source of bleeding during mandibular third molar surgery, yet its true incidence and anatomical characteristics remain controversial due to limitations of conventional imaging. This study aimed to evaluate the detection rates and morphological features of the PMC using four imaging modalities.

Methods

A total of 389 participants (766 mandibular sides) were enrolled and examined using cone-beam computed tomography (CBCT), spiral CT, 3.0T magnetic resonance imaging (MRI), or contrast-enhanced MRI. Detection rates were compared using Fisher–Freeman–Halton exact tests and binary logistic regression.

Results

The detection rate of the PMC increased significantly with improved soft-tissue resolution: 32.37% for CBCT, 63.21% for spiral CT, 80.72% for contrast-enhanced MRI, and 93.75% for 3.0T MRI ($P < 0.001$). High-field MRI consistently revealed a three-branch architecture comprising apical foramen, periodontal ligament, and retromolar branches. The main trunk of the PMC was observed even in patients with congenital absence of the mandibular third molar germ, indicating that the PMC is an inherent anatomical structure rather than a developmental variant.

Conclusions

The PMC is a consistent anatomical feature of the retromolar triangle that has been systematically underestimated by conventional CBCT. Reliance on CBCT alone may lead to underappreciation of surgical bleeding risks during third molar extraction when the canal runs adjacent to the surgical site. Preoperative recognition of this structure, particularly on high-resolution MRI, is clinically relevant for anticipating and managing intraoperative bleeding.

1. Introduction

The posterior molar canal has traditionally been regarded as a rare anatomical variation of the mandibular alveolar nerve canal within the posterior molar triangle. Nonetheless, reports of bleeding incidents resulting from injuries during the extraction of the mandibular third molar occasionally occur, indicating that this structure may possess clinical significance that has yet to be fully acknowledged [1, 2]. The posterior molar triangle is a significant area of interest across various disciplines, including oral surgery, prosthodontics, and orthodontics. This region includes critical structures such as the posterior molar pad, gland, foramen, canal, and retromolar space [1, 3, 4].

Reported incidence rates of the posterior molar canal vary widely in the literature, ranging from 5.4% to 75.4%, with most studies relying on conventional imaging techniques such as panoramic tomography or cone-beam CT (CBCT) [5–7]. Panoramic tomography is limited by image distortion and overlap, which hinder its ability to identify fine anatomical structures [8, 9]. Although cone beam computed tomography (CBCT) has improved the visualization of surgical area details, its advantages primarily pertain to high-contrast imaging of hard tissues. In regions characterized by low density or substantial density variations, the imaging performance remains inadequate [6, 10, 11]. An in-depth exploration is warranted to determine whether the limitations of the aforementioned imaging techniques have resulted in a systematic underestimation of the incidence of posterior molar canals, specifically a relatively high rate of missed detections.

The conventional perspective characterizes the posterior molar canal as a variant branch of the inferior alveolar nerve canal within the posterior molar triangle. however, this interpretation is met with skepticism. Recent studies predominantly propose that the posterior molar canal is an incidental offshoot of the inferior alveolar nerve canal, with a trajectory akin to other variant branches. [12–14]. However, previous clinical observations by our research group indicated that the posterior molar canal consistently exists within the posterior molar triangle, suggesting that it may not be an incidental structure. Additionally, related reports frequently describe mandibular canal injury as presenting with abnormal sensations or numbness in the lower lip and the ipsilateral buccal gingiva following the procedure [15–21]. In the cases of posterior molar tubulo-related injuries examined by our research group, intraoperative bleeding was the primary manifestation. Postoperative numbness and other neurological symptoms were infrequently observed in clinical practice, and in the majority of instances, the affected structure was identified only upon reviewing preoperative imaging data after the procedure. Furthermore, some scholars argue that there is no essential link between the presence of the mandibular third molar and the posterior molar canal. [8, 22], However, after examining pertinent cases, our research group has proposed an alternative perspective. These findings have prompted a reevaluation of the physiological functions and clinical significance of the posterior molar canal.

To address these concerns, our team systematically evaluated the true detection rate and anatomical morphology of the posterior molar canal by comparing three imaging modalities: CBCT, spiral CT, and high-field MRI. Additionally, we preliminarily explored the potential relationship between the composition of the canal's contents, particularly vascular components, and clinical bleeding complications. This study aims to provide imaging evidence that may elucidate the underlying causes of related intraoperative complications.

2. Materials and Methods

2.1. Ethical Review

This study complies with the relevant ethical principles of the Declaration of Helsinki. The research protocol has been reviewed and approved by the Science and Technology Ethics Committee of Xi'an

Medical University (Approval Number: XYLS2025357). All subjects provided written informed consent before participating in the study.

2.2. Experimental Design

This study is a retrospective imaging observational study. The 3.0T MRI data were obtained from volunteers who gave informed consent. The aim was to systematically evaluate and compare the detection rates and morphological characteristics of four imaging techniques - CBCT, spiral CT, 3.0T MRI, and enhanced MRI - for the posterior molar canal.

2.3. Sample Source and Grouping

2.3.1. grouping of observations

A total of 389 participants were enrolled and divided into 4 groups based on imaging modality (Table 1). Group A (CBCT group) consisted of 122 patients who underwent CBCT at the Third Affiliated Hospital of Xi'an Medical University between January 1, 2024 and February 10, 2026. Group B (spiral CT group) comprised 140 volunteers from other ongoing studies in our laboratory who underwent spiral CT scanning. Group C (3.0T MRI group) included 40 randomly selected volunteers from Group B to validate the spiral CT findings. Group D (contrast-enhanced MRI group) consisted of 87 patients who underwent head and neck contrast-enhanced MRI for diagnostic or screening purposes at Shaanxi Provincial Cancer Hospital between January 1, 2024 and March 10, 2026. The overall age range was 18–91 years (mean = 55.25 years).

Table 1
grouping of observations

Group	Imaging technique	Number of cases (n)	Number of the lower jaw side (n)
Group A	CBCT	122	240
Group B	Spiral CT	140	280
Group C	3.0T MRI	40	80
Group D	Enhanced MRI	87	166

2.3.2. Inclusion and Exclusion Criteria

Inclusion criteria

1. Age ≥ 18 years old.
2. Pathological changes without altering the three-dimensional course of the mandibular canal.
3. The image quality is clear, with no severe artifacts interfering with observation.

Exclusion criteria

1. There are pathological conditions that affect the morphology or course of the mandibular canal (such as tumors, cysts, and severe inflammation).
2. There is a clear history of systemic diseases or related medication use that have an impact on bone metabolism..
3. There is a history of mandibular trauma or surgery, resulting in significant changes to the anatomical shape of the mandible..
4. Have a cardiac pacemaker, artificial valve, nerve stimulator, ferromagnetic vascular clips or metallic foreign bodies in the eye (applicable for MRI examination).
5. Patients who are unable to cooperate with the examination due to high fever, coma, altered consciousness, mental abnormalities, prone to epilepsy or cardiac arrest, severe trauma, claustrophobia, or inability to lie flat for more than 30 minutes.

2.3.3. Sample size determination

No formal sample size calculation was performed. All eligible images meeting the inclusion criteria during the specified recruitment periods were included.

2.4. Equipment and Parameters

CBCT equipment model: Rui Li CBCT-RCT700-sc

Scanning parameters: Tube voltage: 90 kVp, Tube current: 5 mA, Scanning thickness: 0.30 mm, Scanning range: 160 mm × 100 mm

Spiral CT equipment model: Lun Imaging uCT 128

Scanning parameters: Scanning tube voltage 140 KV, Tube current 667 mA, Pixel matrix 512 × 512, Layer thickness 0.6 mm, Resolution 0.25 mm^3

MRI equipment model: Siemens MAGNETOM Skyra 3.0T MR

Scanning sequences are shown in Table 2

Table 2
Scanning Sequence

Sequence name	**Spatial resolution**			**Acquisition parameter**		
	Voxel(mm)	**Slice thickness (mm)**	**Interlamellar spacing (mm)**	**TR(ms)**	**TE(ms)**	**average time**
t2_de3d_we_sag_p2_iso	0.6*0.6*0.6	0.58	0	14.84	5.04	2
t2_tse_tra_small fov_320	0.8*0.8*1.0	1.0	0	60.60.0	106.0	5
MPR_Range	0.6*0.6*0.6	0.6	0	14.8	5.0	1

2.5. Research Methods and Image Analysis

Import all DICOM format files of the images into RadiAnt DICOM Viewer (software, Poland, version 2025), and use the 3D multi-planar reconstruction (MPR) function to reconstruct the images.

Two oral surgeons (Doctor A, 26 years of clinical experience, Doctor B, 10 years of clinical experience) who were unaware of the grouping situation independently observed from the coronal, sagittal, and cross-sectional views. The observed contents included::

1. Is the posterior molar canal present (positive/negative)?
2. The course and branching patterns of the posterior molar canals (such as the apical foramen branch, periodontal ligament branch, and posterior molar canal branch)

The images of each subject were observed twice, with an interval of one week, in order to evaluate the consistency within and between observers.

2.6. Statistical Methods

Data analysis was performed using SPSS (software, USA, version 25.0). Count data are presented as both frequencies (n) and percentages (%). The overall detection rate of posterior molar canals among the four imaging modalities (CBCT, spiral CT, 3.0T MRI, and enhanced MRI) was compared using the Fisher-Freeman Halton exact probability method. The Bonferroni correction was applied to adjust the significance level ($\alpha' = 0.0083$) for subsequent pairwise comparisons. The Pearson χ^2 test was utilized for comparisons between group A and group B, while Fisher's exact test was employed for comparisons involving group C (3.0T MRI).

To account for the impact of imaging modality on detection rates, the detection of the posterior molar canal was treated as the dependent variable, with the status of the mandibular third molar (present vs. absent) and the type of imaging equipment as independent variables. A binary logistic regression analysis was conducted. The detection rate for the 3.0T MRI group was 93.75%, with no issues of complete data separation. thus, this group was included in the regression model. Variables were selected using the entry method, and the odds ratio (OR) along with its 95% confidence interval (CI) was calculated.

Further evaluate the interaction between the type of equipment and the state of the mandibular third molar. Incorporate the product term of these two variables into the regression model and utilize the likelihood ratio test to assess the significance of the interaction ($P < 0.05$).

Based on this analysis, a stratified evaluation was performed to examine the association between the state of the mandibular third molar and the detection of the posterior molar canal, categorized by different imaging devices. The Pearson χ^2 test or Fisher's exact test was employed for the CBCT, spiral CT, and enhanced MRI groups. In the 3.0T MRI group, given that the detection rates for both categories were relatively high (90.48% for the presence group and 97.37% for the absence group), Fisher's exact

test was also applied for intra-group comparison. All tests were two-tailed, and a difference of $P < 0.05$ was deemed statistically significant.

No missing data were present for the primary outcome variables in this study. All enrolled participants had complete imaging data available for analysis.

No sensitivity analyses were conducted because the main analyses were based on complete data without imputation.

3. Experimental Results and Analysis

3.1. Observation of the posterior molar canals of molars under different imaging methods

3.1.1. Comparison of Detection of Posterior Tooth Canal by Spiral CT and 3.0T MRI

For the subjects whose posterior molar canal was not detected by spiral CT, further 3.0T MRI examination was conducted. The results showed that in this group of subjects, the posterior molar canal structure was clearly displayed in 3.0T MRI (Figs. 1a and 1d). while in the subjects whose posterior molar canal was detected by spiral CT, the pipeline course shown by the two imaging techniques was highly consistent (Figs. 1b and 1e). at the same time, some subjects were not detected with the posterior molar canal in both spiral CT and 3.0T MRI examinations (Figs. 1c and 1f).

a Subject 1, female, 22 years old, sagittal MPR reconstruction of spiral CT image of the right mandible (spiral CT negative). b Subject 2, male, 23 years old, sagittal MPR reconstruction of spiral CT image of the right mandible (spiral CT positive). c Subject 3, male, 23 years old, sagittal MPR reconstruction of spiral CT image of the left mandible (spiral CT negative). d Subject 1, female, 22 years old, sagittal MPR reconstruction of 3.0T MRI t2_tse_tra_small fov_320 sequence image (MRI positive). e Subject 2, male, 23 years old, sagittal MPR reconstruction of 3.0T MRI t2_tse_tra_small fov_320 sequence image (MRI positive). f Subject 3, male, 23 years old, sagittal MPR reconstruction of 3.0T MRI image, no posterior mandibular canal structure was observed (MRI negative)

3.1.2. Comparison of the morphology of the posterior molar canals under different imaging methods

When the morphology of the posterior molar canal was examined using different imaging modalities, it became evident that most posterior molar canals are not single channels. As shown in Fig. 2, 3.0T MRI and contrast-enhanced MRI — owing to their superior ability to differentiate soft tissues and blood vessels — clearly revealed a three-branch architecture: the apical foramen branch, which terminates at the apical foramen of the last molar; the periodontal ligament branch, which terminates at the periodontal membrane; and the retromolar branch, which terminates in the retromolar region.

a Subject 3, male, 62 years old, sagittal MPR reconstruction of CBCT image of the right mandible. b Subject 3, female, 22 years old, sagittal MPR reconstruction of spiral CT image of the left mandible. c Subject 4, female, 22 years old, sagittal MPR reconstruction of 3.0T MRI t2_tse_tra_small fov_320 sequence image. d Subject 5, female, 23 years old, sagittal MPR reconstruction of 3.0T MRI MPR_Range sequence image of the right mandible. e Subject 6, female, 46 years old, enhanced MRI sagittal MPR reconstruction of the left mandible.

3.1.3. The performance of the posterior molar canals of the same patient under different detection methods

To eliminate the interference caused by individual anatomical variations, the images of two sequences (CBCT, spiral CT, and 3.0T MRI) of the same subject (with the third molar present in the mandible) were compared (Fig. 3). The results showed that CBCT (Fig. 3a) could observe a branch starting from the mandibular canal and extending towards the root of the third molar, but no secondary branches were seen. spiral CT (Fig. 3b) showed good continuity of the pulp chamber of the posterior mandibular canal, but still could not distinguish the fine branches. the 3.0T MRI T2_TSE_tra_small FOV_320 sequence (Fig. 3c) and MPR_Range sequence (Fig. 3d) further presented the typical three-branch structure through multi-planar reconstruction - the apical foramen branch, the periodontal ligament branch, and the posterior pulp chamber branch.

a The reconstructed CBCT image of the right mandibular body in sagittal view for subject 6, female, 23 years old. b Spiral CT image. c 3.0T MRI t2_tse_tra_small fov_320 sequence image. d 3.0T MRI MPR_Range sequence image

3.2. Detection Rate and Statistical Analysis of Post-Molar Canal in Four Groups of Images

The detection results of the posterior molar canal using four imaging techniques are shown in Table 3. The detection rate of CBCT (Group A) was 32.37%. that of spiral CT (Group B) was 63.21%. the detection rate of 3.0T MRI (Group C) was as high as 93.75%. and the detection rate of enhanced MRI (Group D) was 80.72%.

Table 3
Detection of Post-Molar Canals in Different Imaging Groups

Group	Imaging technique	Number of observation sides (n)	Positive side count (n)	Detection rate (%)
Group A	CBCT	240	78	32.37
Group B	Spiral CT	280	177	63.21
Group C	3.0T MRI	80	75	93.75
Group D	Enhance MRI	166	134	80.72

The inter-observer and intra-observer consistency was evaluated using the Kappa test. The results showed that the inter-observer Kappa values for CBCT, spiral CT, 3.0T MRI, and enhanced MRI were 0.82 (95% CI: 0.75–0.89), 0.79 (95% CI: 0.71–0.87), 0.91 (95% CI: 0.84–0.98), and 0.85 (95% CI: 0.78–0.92), respectively. All of these values indicated good consistency (Kappa > 0.75). The intra-observer Kappa values ranged from 0.82 to 0.94, all higher than 0.80.

The Fisher-Freeman-Halton exact probability method was used to compare the detection rates of the four groups, and the difference was statistically significant ($P < 0.001$). After Bonferroni correction ($\alpha' = 0.0083$), the detection rate of 3.0T MRI was significantly higher than that of CBCT ($P < 0.001$) and spiral CT ($P < 0.001$), but there was no statistically significant difference compared with enhanced MRI ($P = 0.032$). there was no statistically significant difference in the detection rates between enhanced MRI and spiral CT ($P = 0.089$), and both were significantly higher than that of CBCT ($P < 0.001$).

3.3 Study on the Relationship between the Posterior Canal of the Molar and the Mandibular Third Molar

The distribution of PMC detection and mandibular third molar status across the four imaging systems is shown in Table 4.

Table 4
Distribution of the detection of the posterior molar canals and the status of the mandibular third molars in the four imaging systems

Group	Imaging technique	Mandibular third molar	Molar posterior canal		aggregate
			positive	negative	
Group A	CBCT	exist	39	66	105
		deficiency	39	96	135
Group B	Spiral CT	exist	140	70	210
		deficiency	37	33	70
Group C	3.0T MRI	exist	38	4	42
		deficiency	37	1	38
Group D	Enhance MRI	exist	73	14	87
		deficiency	62	17	79

3.3.1 Group Analysis: The Association between the Status of the Mandibular Third Molar in Each Device and the Detection of the Post-Molar Canal

Table 5
Correlation Analysis of the Status of the Mandibular Third Molar and the Detection of Post-Molar Canal in Various Imaging Equipment Groups

Group	**Imaging technique**	**Detection rate (presence vs absence)**	**OR(95%CI)**	**χ^2**	***P*-value**
Group A	CBCT	37.14% vs 28.89%	1.45(0.85–2.48)	1.866	0.172
Group B	Spiral CT	69.54% vs 56.25%	1.78(0.98–3.21)	3.670	0.055
Group C	3.0T MRI	90.48% vs 97.37%	0.26(0.03–2.39)	—	0.3541
Group D	Enhance MRI	83.91% vs 77.22%	1.54(0.72–3.29)	1.220	0.269

The stratified analysis results are summarized in Table 5. Within each imaging device group, the rate of detecting the posterior canal of the third molar in those with the molar present was higher than that in those with the molar absent (except for group C), but the differences were not statistically significant ($P > 0.05$).

3.3.2. Inter-group comparison: The overall detection capability of different imaging devices for the posterior molar canals of molars

Using CBCT as the reference, a binary logistic regression was conducted (dependent variable: whether the posterior molar canal was detected; independent variable: type of imaging equipment; correction of wisdom teeth status). The results are presented in Table 6. After correcting for the status of the mandibular third molar, spiral CT, 3.0T MRI, and enhanced MRI all had significantly better detection capabilities for the posterior molar canal than CBCT ($P < 0.001$).

Table 6
Overall detection ability of posterior molar canals by different imaging equipment

Group	Imaging technique	OR	95% CI	*P-value*
Group B	Spiral CT	3.36	2.32–4.87	<0.001
Group C	3.0T MRI	27.65	12.38–61.74	<0.001
Group D	Enhance MRI	8.15	4.83–13.75	<0.001

Binary logistic regression model was used. The dependent variable was the detection of the posterior molar canal (1 = detected, 0 = not detected), and the independent variables were the type of imaging equipment (with CBCT as the reference) and the status of the mandibular third molar (present/absent).

The results showed that after correcting for the status of the mandibular third molar, spiral CT, 3.0T MRI, and enhanced MRI all had significantly better detection capabilities for the posterior molar canal than CBCT ($P < 0.001$)

3.3.3. Interaction Test

To assess whether the type of imaging equipment has an effect-modifying effect on the association between "status of the third molar of the mandible" and "detection of the posterior molar canal", the product term of "imaging equipment type × status of the third molar of the mandible" was included in the binary logistic regression model, and the interaction analysis was conducted using the likelihood ratio test. All four sets of data were included in the model. The results showed that the interaction was statistically significant ($\chi^2 = 8.96$, $P = 0.030$), suggesting that there are significant differences in the impact of the third molar of the mandible on the detection of the posterior molar canal under different imaging equipment, and the equipment type is the effect-modifying factor for this association.

4. Conclusion

This study demonstrates that the posterior molar canal is an inherent anatomical structure rather than a rare variation, consistently identifiable within the posterior molar triangle. The detection rates of this structure differ across imaging modalities: 32.5% for cone-beam computed tomography (CBCT), 63.2% for spiral computed tomography (CT), 93.8% for 3.0T magnetic resonance imaging (MRI), and 80.7% for enhanced MRI ($P < 0.001$). The superior detection capability of high-field MRI compared to CBCT indicates that conventional imaging techniques may systematically underestimate the true prevalence of

this anatomical feature. Among the detectable cases, the posterior molars exhibit a consistent three-branch morphology, comprising the apical foramen branch, the periodontal ligament branch, and the posterior molars foramen branch. The presence of the main branch is independent of the mandibular third molars. however, the secondary branches are more frequently observed when the third molars are present. Clinically, if the main trunk of the posterior molar canal runs superficially or is adjacent to the surgical site during the extraction of the mandibular third molar, this anatomical feature may pose a potential source of intraoperative bleeding. Although cone beam computed tomography (CBCT) remains the standard for preoperative imaging assessment, clinicians should recognize that its limited sensitivity to the posterior molar canal may result in an underestimation of surgical risks.

5. Discussion

Scholars have undertaken comprehensive anatomical investigations of the posterior molar triangle, focusing specifically on the characteristics of blood vessels and nerves in this region[1]. It is widely accepted that a distinct bony canal, known as the posterior molar canal, is present in this area. This canal contains vascular and nerve bundles that are associated with one or more variant branches of the inferior alveolar neurovascular bundle [17, 23]. According to statistics, the detection rate of this neural vascular bundle in CBCT ranges from 5.4% to 75.4% [9]. In this study, spiral CT and high-field MRI were used for detection. The results showed that the detection rate of the posterior molar canal could be as high as 93.75% (3.0T MRI), and the detection rates in spiral CT and enhanced MRI were 63.21% and 80.72% respectively, both of which were higher than the detection rate of CBCT (32.37%) in this study. Some scholars have classified the vascular nerve bundles in this area in further research [12]: Type I (posterior molar canal) opens in the posterior molar region. Type II (dental canal) extends toward the root of the mandibular third molar. Type III (anterior canal) runs parallel to the main trunk of the mandibular canal. and Type IV (buccal-lingual canal) penetrates the buccal or lingual bone plate. Types I, II, and IV are confined to the posterior molar triangle area and should be classified as part of the posterior molar canal under discussion. In contrast, Type III (anterior canal) represents a variant fork of the mandibular canal, with its insertion point located far from the posterior molar area or rejoining the main canal of the mandibular canal. We assert that the posterior molar canal should not be grouped together with other mandibular canal branches. The latter should be classified at the same anatomical level and more appropriately referred to collectively as "mandibular canal bifurcations," which are parallel structures of the mandibular canal. In this discussion, we define the "posterior molar canal" as the first branch of the mandibular canal within the posterior molar area.

Previous studies in stomatology primarily utilized conventional imaging methods, including curved surface tomography and cone-beam computed tomography (CBCT), the latter of which has gained widespread adoption in recent years [9, 24, 25]. In studies focusing on specific anatomies or lesions, including tumors in the posterior molar region, hemangiomas in the jawbone, and thick branches of the mandibular canal, some researchers have employed spiral computed tomography (CT) or magnetic resonance imaging (MRI) [26–28], This study relies on a significant reference. Cone beam computed tomography (CBCT) offers superior imaging for high-contrast hard tissues. however, its quality remains

limited in regions characterized by low density or substantial density variations[29, 30]. In contrast, spiral computed tomography (CT) provides enhanced density resolution, allowing for clearer visualization of soft tissues, blood vessels, and structures with similar densities[31–33]. This capability facilitates the differentiation of tissues with varying densities, thereby yielding more comprehensive diagnostic information [2]. Leveraging the advantages of spiral computed tomography (CT), this study initially employed spiral CT to evaluate the imaging rate of the posterior molar canal. The detection rate of the posterior molar canal using cone-beam computed tomography (CBCT) was found to be 32.37%, whereas spiral CT achieved a detection rate of 63.21%. This finding further underscores the superiority of spiral CT in identifying low-density structures, including nerves and blood vessels. Additionally, the trabecular bone structure is distinctly visible in CT images, particularly the trabecular bone that aligns parallel to the branches of the mandibular canal, which often significantly obstructs the observation of this canal. To mitigate the interference caused by such bony artifacts, this experiment incorporated magnetic resonance imaging (MRI) technology, providing an effective supplementary approach for identifying the mandibular canal and its branches [34–36]. Leveraging the advantages of spiral computed tomography (CT), this study initially employed spiral CT to evaluate the imaging rate of the posterior molar canal. The detection rate of the posterior molar canal using cone-beam computed tomography (CBCT) was found to be 32.37%, whereas spiral CT achieved a detection rate of 63.21%. This finding further underscores the superiority of spiral CT in identifying low-density structures, including nerves and blood vessels. Additionally, the trabecular bone structure is distinctly visible in CT images, particularly the trabecular bone that aligns parallel to the branches of the mandibular canal, which often significantly obstructs the observation of this canal. To mitigate the interference caused by such bony artifacts, this experiment incorporated magnetic resonance imaging (MRI) technology, providing an effective supplementary approach for identifying the mandibular canal and its branches.

During the observation process, we also noted that the posterior molars of most subjects did not exhibit single channels. instead, they displayed branches and other conformations. However, individual differences and imaging limitations contributed to considerable variability in these findings. Magnetic resonance imaging (MRI), known for its high sensitivity to neurovascular structures, can clearly delineate the course and distribution of the inferior alveolar artery and its smaller branches [32, 37]. We further examined the morphological characteristics of the small arteries within the posterior molar canal. In most subjects, the branching structure of the inferior alveolar artery was distinctly visible, and its trajectory aligned with the main trunk direction of the posterior molar canal, accompanied by secondary branches. This observation suggests that the distribution pattern of arterial branches reflects the complexity of the bony ducts in which they reside, indicating the presence of corresponding branches or accompanying ducts in the posterior molars. This finding supports the notion that the majority of subjects possess the posterior molar canal as an anatomical structure. Notably, even in images of patients with absent mandibular third molars, the posterior molar canal remains discernible. This result further substantiates the hypothesis that the posterior molar canal may represent a universal physiological structure. In certain MRI images, it is evident that the small arteries within the posterior molar canal do not consist solely of a single main trunk originating from the inferior alveolar artery and terminating at the posterior molar foramen in the posterior molar region. Most small arteries observed in

the posterior molar canal exhibit two branches: the apical branch, which terminates at the apical foramen of the lower jaw's last molar, and the periodontal ligament branch, which concludes at the periodontal ligament of the same molar (Fig. 4). We hypothesize that in cases where the lower jaw's third molar is absent, the aforementioned secondary branches may regress or vanish, leaving only the main trunk to extend to the posterior molar gland.

During the 3.0T MRI examination, this study identified two cases of particular anatomical significance, offering insights into the developmental relationship between the posterior molar canal and the mandibular third molar. These two cases are shown in Fig. 5. Case One involved a patient with a congenital absence of the mandibular third molar germ. The MRI image distinctly revealed the structure of the posterior molar canal, suggesting that its presence may not be contingent upon the development of the third molar. Case Two featured a patient whose mandibular third molar was in the early stages of development, with the root not yet fully formed. The MRI image for this patient also clearly depicted the posterior molar canal structure, indicating that its formation can occur during the early developmental phase of the third molar and is not reliant on the complete maturation of the root. To further validate the universality of the aforementioned observations, this study employed a stratified analysis method to assess the relationship between the condition of the mandibular third molar and the detection of the posterior molar canal, categorized by type of imaging equipment. The results indicated that among the four groups of imaging devices, the detection rate of posterior molar canals in individuals with mandibular third molars was higher than in those with absent molars. This trend exhibited a high degree of consistency across all four imaging techniques. Under high-field MRI, the posterior molar canal exhibits an exceptionally high detection rate, regardless of the presence of the third molar, with rates of 90.48% in the presence group and 97.37% in the absence group. This finding suggests that the main trunk of this structure may represent an inherent anatomical feature of the posterior molar triangle, independent of third molar development. The detection rate in the presence group was slightly higher than that in the absence group, potentially due to the increased branching of secondary structures, such as apical foramen branches and periodontal ligament branches, when the third molar is present. These additional branches are more readily identifiable in conventional imaging, thereby enhancing the overall detection rate. Based on case observations and statistical trends, this study offers the following preliminary insights: The posterior molar canal represents a relatively fixed anatomical structure within the posterior molar triangle. The presence of its main trunk does not appear to depend on the mandibular third molar. rather, it is closely associated with the blood supply requirements of the surrounding soft tissues, such as the posterior molar gland. In cases where the mandibular third molar is present, this canal can further differentiate into apical foramen branches and periodontal ligament branches, thereby providing vascular and nerve support to the tooth root and periodontal tissues. Conversely, when the mandibular third molar is absent, only the main trunk may persist, extending towards structures like the posterior molar gland. The aforementioned inference remains a preliminary understanding. Future research should aim to increase the sample size, incorporate additional cases of congenital absence of the third molar and incomplete root development, and integrate multimodal imaging with histological analysis. This approach will further elucidate the developmental mechanisms of the posterior molar canal and its spatiotemporal relationship with the mandibular third molar.

a. MRI image of the right mandible of subject 6 at 3.0T. b. MRI image of the left mandible of subject 6 at 3.0T.

c MRI image of the right mandible of subject 7 at 3.0T. d MRI image of the left mandible of subject 7 at 3.0T.

The anatomical structure of the posterior molar canal branches is likely to serve a distinct physiological function, analogous to the nourishing blood vessels that extend to each molar during the course of the mandibular canal, which runs from the mandibular foramen to the mental foramen. Notably, in the third mandibular molar, these two branches arise from the vascular nerve bundles within the posterior molar canal, rather than from the main trunk. Currently, there is a paucity of systematic analysis regarding the blood supply and neural innervation of both soft and hard tissues in the posterior molar region. For example, the neural origins of the posterior molar glands, as well as the distribution of blood vessels and nerves within the periodontal ligament of the third molar, remain poorly understood. Given the intricate anatomical structure and significant functional relevance of this area, it is reasonable to expect a relatively stable source of vascular nerves. Considering both positional and morphological aspects of the branches, the posterior molar canal, which exhibits a relatively high incidence rate, is likely to play a crucial role in this context.

Through an examination of actual clinical medical records, we observed that during tooth extraction, the neurovascular bundle at the posterior foramina of the molar is frequently severed while creating the flap to expose the surgical field. This occurrence can be attributed to its superficial location, limited blood flow, and the fact that gingival sensation in this region is regulated by both the inferior alveolar nerve and the long buccal nerve [38]. Postoperatively, only mild or no significant numbness is typically observed, accompanied by minimal bleeding that is easily controlled. In contrast, the secondary branches responsible for innervating the periodontal ligament and the apical foramen are situated deeper and in closer proximity to the mandibular canal, where blood flow is more substantial. If these branches are severed during the procedure, the resultant bleeding is more pronounced, often presenting as rapid blood ejection or pinpoint bleeding following bone removal and space expansion with the turbine handpiece. Although such bleeding rarely poses a life-threatening risk, achieving hemostasis can be considerably more challenging. We hypothesize that in patients experiencing this type of bleeding, preoperative CBCT often reveals a distinct branch of the mandibular canal (i.e., the visible posterior molar canal), and damage to this branch may primarily account for bleeding during the extraction of the mandibular third molar, aside from potential injury to the mandibular canal itself. However, injuries to the posterior molar canal are generally infrequent. A significant portion of intraoperative bleeding still arises from damage to the main mandibular canal. Accidental injury to the main posterior molar canal is more likely to occur when it runs superficially or is adjacent to the surgical site. For the visible posterior molar canal identified through cone-beam computed tomography (CBCT), the surgeon must exercise caution and refrain from excessive bone removal in the area it traverses. If necessary, an ultrasonic bone knife may be employed to minimize tissue damage, or the patient can be referred to a specialized facility equipped for more effective hemostasis[39]. Regarding hidden posterior molars detectable only via magnetic resonance

imaging (MRI) and not visible on CBCT, the current imaging modalities are not routinely employed for this purpose, thereby limiting their clinical significance. Nevertheless, there is variability in the proposed branching patterns of the mandibular canal. Ultimately, in the absence of higher-precision imaging technologies, meticulous interpretation of existing CBCT images and the avoidance of overlooking critical anatomical details are essential for ensuring surgical safety.

The limitations of objective conditions have resulted in a relatively small dataset in this study, making it challenging to validate the universality of the aforementioned theory. Furthermore, as a preliminary exploratory study, the generalisability of these findings is limited to the Chinese population, as all participants were recruited from two institutions in Shaanxi Province, China, and were predominantly of Chinese Han ethnicity. Whether these findings extend to other ethnic groups or geographic regions remains unknown. Future research should aim to expand both the sample size and the sources of samples, with an emphasis on increasing the number of cases in the MRI plain scan and enhanced control groups. Multicentre studies incorporating diverse ethnic populations are warranted to validate the external validity of these observations. This approach will further assess the diagnostic efficacy of various imaging techniques for the posterior molar region. Concurrently, investigations should track imaging changes before and after the extraction of wisdom teeth. Additionally, the imaging capabilities of ultra-high field strength MRI or micro-CT for latent branches warrant exploration. By integrating multimodal imaging with surgical findings, this research aspires to systematically elucidate the complete anatomical lineage of this vascular nerve bundle and its clinical implications.

Declarations

Declaration of competing interest:

The authors declared no potential conflicts of interest with respect to the research, authorship, and/or publication of this article.

Ethical approval:

This study complies with the relevant ethical principles of the Declaration of Helsinki. The research protocol has been reviewed and approved by the Science and Technology Ethics Committee of Xi'an Medical University (Approval Number: XYLS2025357). All subjects provided written informed consent before participating in the study.

Funding:

This work was supported by the Shaanxi Provincial Health Research Innovation Capacity Enhancement Program (Grant No. 2025YF-44).

Author Contribution

Bolun Zhang and Siyu He contributed equally to this work as co first authors. Bolun Zhang and Siyu He were responsible for conceptualization, methodology, writing the original draft, and visualization. Yuan Li and Zhuolin Han performed data curation and formal analysis, and contributed to writing – review and editing. Su Liu, Lihao Zhang, and Xingxing Mu were responsible for investigation and resource acquisition (CBCT, spiral CT, and contrast enhanced MRI), and contributed to writing – review and editing. Fei Liang and Kaijin Hu contributed equally as co corresponding authors. Fei Liang was responsible for conceptualization, funding acquisition, project administration, supervision, and writing – review and editing. Kaijin Hu was responsible for conceptualization, methodology, resources, supervision, and writing – review and editing. All authors reviewed and approved the final manuscript and agree to be accountable for all aspects of the work.

Acknowledgments:

The authors thank all participants and staff involved in this study. The imaging methodologies and data processing frameworks employed in this study were partially supported by the above-mentioned funding. The authors gratefully acknowledge the contributors who facilitated the image acquisition and data management.

References

1. Sisman Y, Ercan-Sekerci A, Payveren-Arikan M, Sahman H. Diagnostic accuracy of cone-beam CT compared with panoramic images in predicting retromolar canal during extraction of impacted mandibular third molars. Med Oral Patol Oral Cir Bucal. 2015;20(1):e74–81.
2. Ueno D, Sato J, Igarashi C, Ikeda S, Morita M, Shimoda S, Udagawa T, Shiozaki K, Kobayashi M, Kobayashi K. Accuracy of oral mucosal thickness measurements using spiral computed tomography. J Periodontol. 2011;82(6):829–36.
3. Shah SP, Mehta D. Mandibular Retromolar Foramen and Canal - A Systematic Review and Meta-Analysis. Ann Maxillofac Surg. 2020;10(2):444–9.
4. Park MK, Jung W, Bae JH, Kwak HH. Anatomical and radiographic study of the mandibular retromolar canal. J Dent Sci. 2016;11(4):370–6.
5. Patil S, Matsuda Y, Nakajima K, Araki K, Okano T. Retromolar canals as observed on cone-beam computed tomography: their incidence, course, and characteristics. Oral Surg Oral Med Oral Pathol Oral Radiol. 2013;115(5):692–9.
6. Han SS, Hwang YS. Cone beam CT findings of retromolar canals in a Korean population. Surg Radiol Anat. 2014;36(9):871–6.
7. Kikuta S, Iwanaga J, Nakamura K, Hino K, Nakamura M, Kusukawa J. The retromolar canals and foramina: radiographic observation and application to oral surgery. Surg Radiol Anat.

2018;40(6):647–52.
8. Ossenberg NS. Retromolar foramen of the human mandible. Am J Phys Anthropol. 1987;73(1):119–28.
9. Truong MK, He P, Adeeb N, Oskouian RJ, Tubbs RS, Iwanaga J. Clinical Anatomy and Significance of the Retromolar Foramina and Their Canals: A Literature Review. Cureus. 2017;9(10):e1781.
10. Salem D, Reher P, Evans JL, Mansour MH. Exploring digital technologies used in the design and manufacture of craniofacial implant surgical guides: A scoping review. J Prosthet Dent. 2024;131(6):1264–70.
11. Li X, Zhang Y, Shi Y, Wu S, Xiao Y, Gu X, Zhen X, Zhou L. Comprehensive evaluation of ten deformable image registration algorithms for contour propagation between CT and cone-beam CT images in adaptive head & neck radiotherapy. PLoS ONE. 2017;12(4):e0175906.
12. Naitoh M, Hiraiwa Y, Aimiya H, Ariji E. Observation of bifid mandibular canal using cone-beam computerized tomography. Int J Oral Maxillofac Implants. 2009;24(1):155–9.
13. Ogawa A, Fukuta Y, Nakasato H, Nakasato S. Evaluation by dental cone-beam computed tomography of the incidence and sites of branches of the inferior dental canal that supply mandibular third molars. Br J Oral Maxillofac Surg. 2016;54(10):1116–20.
14. Iwanaga J, Takeshita Y, Matsushita Y, Hur M-S, Ibaragi S, Tubbs RS. What are the retromolar and bifid/trifid mandibular canals as seen on cone-beam computed tomography? Revisiting classic gross anatomy of the inferior alveolar nerve and correcting terminology. Surg Radiol Anat. 2021;44(1):147–56.
15. Vranckx M, Geerinckx H, Gaêta-Araujo H, Leite AF, Politis C, Jacobs R. Do anatomical variations of the mandibular canal pose an increased risk of inferior alveolar nerve injury after third molar removal? Clin Oral Investig. 2022;26(1):931–7.
16. Singh S. Aberrant buccal nerve encountered at third molar surgery. Oral Surg Oral Med Oral Pathol. 1981;52(2):142.
17. von Arx T, Bornstein MM, Werder P, Bosshardt D. [The retromolar canal (foramen retromolare). Overview and case report]. Schweiz Monatsschr Zahnmed. 2011;121(9):821–34.
18. Kuczynski A, Kucharski W, Franco A, Westphalen FH, de Lima AA, Fernandes A. Prevalence of bifid mandibular canals in panoramic radiographs: a maxillofacial surgical scope. Surg Radiol Anat. 2014;36(9):847–50.
19. Soman C, Wahass T, Alahmari H, Alamri N, Albiebi A, Alhabashy M, Talha A, Alqhtani N. Prevalence and Characterization of bifid mandibular Canal Using Cone Beam Computed Tomography: A Retrospective Cross-Sectional Study in Saudi Arabia. Clin Cosmet Invest Dentistry. 2022;14:297–306.
20. He H, Ruan N. Factors influencing inferior alveolar nerve injury after extraction of mandibular third molar. Med Oral Patología Oral y Cir Bucal 2024:e613–9.
21. C Q, Y N ML. Mandibular Impacted Teeth Closely Attached to the Posterior Canal of Molars: A Case Report. J Oral Sci Res. 2024;40(10):934–7.

22. Nikkerdar N, Golshah A, Norouzi M, Falah-Kooshki S. Incidence and Anatomical Properties of Retromolar Canal in an Iranian Population: A Cone-Beam Computed Tomography Study. Int J Dent. 2020;2020:9178973.
23. Motamedi MH, Gharedaghi J, Mehralizadeh S, Navi F, Badkoobeh A, Valaei N, Azizi T. Anthropomorphic assessment of the retromolar foramen and retromolar nerve: anomaly or variation of normal anatomy? Int J Oral Maxillofac Surg. 2016;45(2):241–4.
24. Yamashita-Mikami E, Tanaka M, Sakurai N, Yamada K, Ohshima H, Nomura S, Ejiri S. Microstructural Observation with MicroCT and Histological Analysis of Human Alveolar Bone Biopsy from a Planned Implant Site A Case Report. Open Dentistry J 2013.
25. Liang RZ, Wu JT, Wu YN, Smales RJ, Hu M, Yu JH, Zhang GD. Bilateral maxillary fused second and third molars: a rare occurrence. Int J Oral Sci. 2012;4(4):231–4.
26. Beck F, Austermann S, Bertl K, Ulm C, Lettner S, Toelly A, Gahleitner A. Is MRI a viable alternative to CT/CBCT to identify the course of the inferior alveolar nerve in relation to the roots of the third molars? Clin Oral Investig. 2021;25(6):3861–71.
27. Marcello Scotti F, Stuepp RT, Leonardi Dutra-Horstmann K, Modolo F, Gusmão Paraiso Cavalcanti M. Accuracy of MRI, CT, and Ultrasound imaging on thickness and depth of oral primary carcinomas invasion: a systematic review. Dentomaxillofacial Radiol 2022, 51(5).
28. Rumboldt Z, Castillo M, Smith JK. The palatovaginal canal: can it be identified on routine CT and MR imaging? AJR Am J Roentgenol. 2002;179(1):267–72.
29. Weiss E, Wu J, Sleeman W, Bryant J, Mitra P, Myers M, Ivanova T, Mukhopadhyay N, Ramakrishnan V, Murphy M, et al. Clinical Evaluation of Soft Tissue Organ Boundary Visualization on Cone-Beam Computed Tomographic Imaging. Int J Radiation Oncology*Biology*Physics. 2010;78(3):929–36.
30. Hall WA, Paulson E, Li XA, Erickson B, Schultz C, Tree A, Awan M, Low DA, McDonald BA, Salzillo T, et al. Magnetic resonance linear accelerator technology and adaptive radiation therapy: An overview for clinicians. CA Cancer J Clin. 2022;72(1):34–56.
31. Gorolay VV, Tran NA, Tade R, Baugnon K, Aiken A, Wu X. The ptotic tongue-imaging appearance and pathology localization along the course of the hypoglossal nerve. Neuroradiology. 2023;65(10):1425–38.
32. Rindler RS, Allen JW, Barrow JW, Pradilla G, Barrow DL. Neuroimaging of Intracerebral Hemorrhage. Neurosurgery. 2020;86(5):E414–23.
33. Parker M, Beyea S, Rioux J, King B, Abdolell M, Reeve S, Lieuwen B, Bowen C, Volders D. 0.5T MRI as a competitor to CT for sinus imaging. Sci Rep. 2024;14(1):31774.
34. Gaudino C, Cosgarea R, Heiland S, Csernus R, Beomonte Zobel B, Pham M, Kim T-S, Bendszus M, Rohde S. MR-Imaging of teeth and periodontal apparatus: an experimental study comparing high-resolution MRI with MDCT and CBCT. Eur Radiol. 2011;21(12):2575–83.
35. Gorolay VV, Tran N-A, Tade R, Baugnon K, Aiken A, Wu X. The ptotic tongue—imaging appearance and pathology localization along the course of the hypoglossal nerve. Neuroradiology. 2023;65(10):1425–38.

36. Kim M, Kang TW, Cha DI, Jang KM, Kim YK, Kim SH, Sinn DH, Kim K. Identification of Arterial Hyperenhancement in CT and MRI in Patients with Hepatocellular Carcinoma: Value of Unenhanced Images. Korean J Radiol 2019, 20(2).
37. Burmeister HP, Baltzer PAT, Klingner CM, Pantel M, Kaiser WA. Computer- und Magnetresonanztomographie des N. facialis. Hno. 2010;58(5):433–42.
38. Svensson P, Mark Drangsholt, Pfau DB, List T. Neurosensory testing of orofacial pain in the dental clinic. Free PMC article 2012.
39. Ye Z-X, Qian W-H, Wu Y-B, Yang C. Comparison of two surgical techniques for the extraction of mandibular horizontally impacted third molars near the mandibular canal: the displacement reduction method and the away-from-nerve method. Clin Oral Invest 2025, 29(6).

Figures

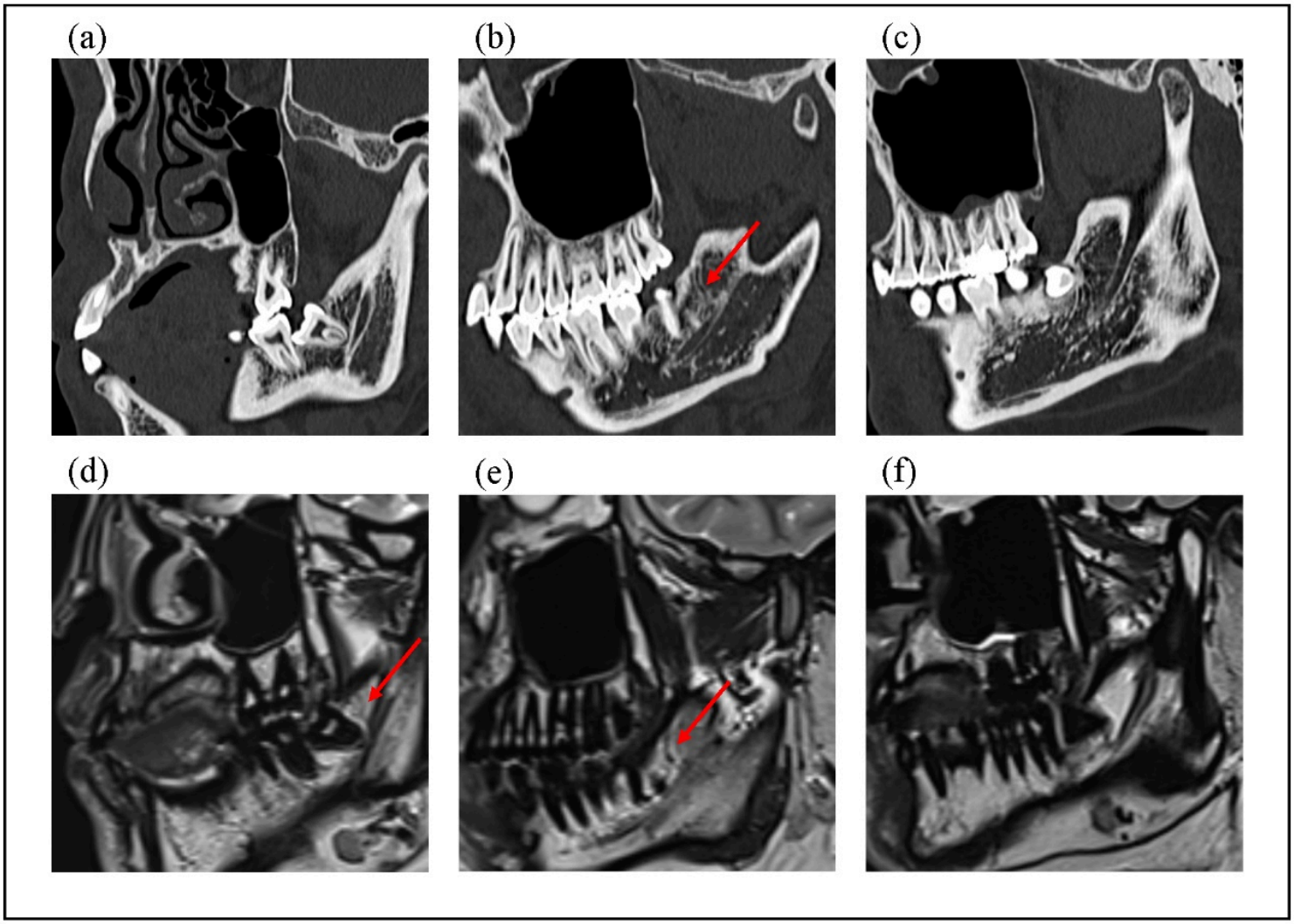


Figure 1

Comparison of detection of the posterior mandibular canal by spiral CT and 3.0T MRI

a Subject 1, female, 22 years old, sagittal MPR reconstruction of spiral CT image of the right mandible (spiral CT negative). b Subject 2, male, 23 years old, sagittal MPR reconstruction of spiral CT image of the right mandible (spiral CT positive). c Subject 3, male, 23 years old, sagittal MPR reconstruction of spiral CT image of the left mandible (spiral CT negative). d Subject 1, female, 22 years old, sagittal MPR reconstruction of 3.0T MRI t2_tse_tra_small fov_320 sequence image (MRI positive). e Subject 2, male, 23 years old, sagittal MPR reconstruction of 3.0T MRI t2_tse_tra_small fov_320 sequence image (MRI positive). f Subject 3, male, 23 years old, sagittal MPR reconstruction of 3.0T MRI image, no posterior mandibular canal structure was observed (MRI negative)

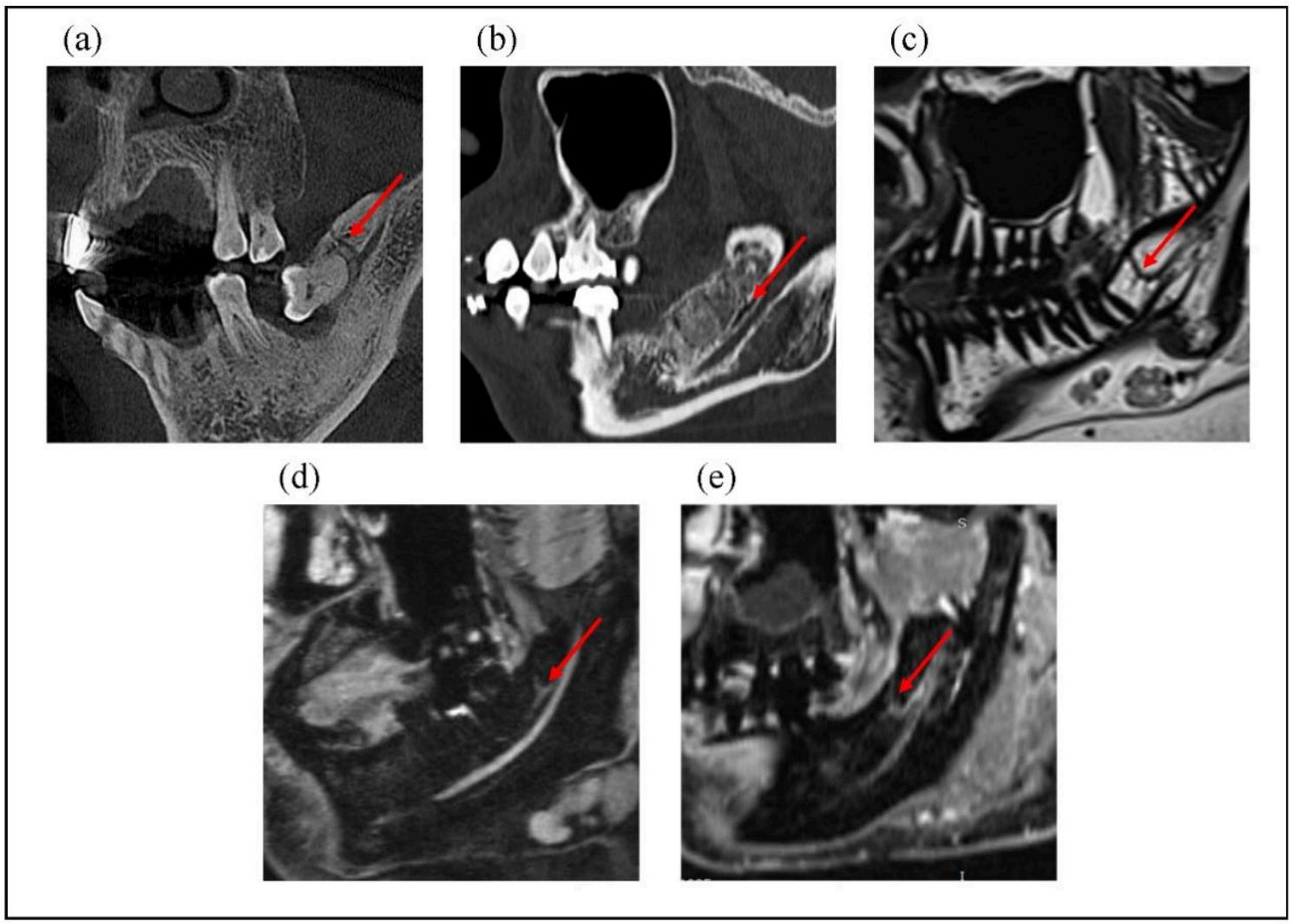


Figure 2

Morphology of the posterior mandibular canal under different imaging methods

a Subject 3, male, 62 years old, sagittal MPR reconstruction of CBCT image of the right mandible. b Subject 3, female, 22 years old, sagittal MPR reconstruction of spiral CT image of the left mandible. c Subject 4, female, 22 years old, sagittal MPR reconstruction of 3.0T MRI t2_tse_tra_small fov_320 sequence image. d Subject 5, female, 23 years old, sagittal MPR reconstruction of 3.0T MRI MPR_Range

sequence image of the right mandible. e Subject 6, female, 46 years old, enhanced MRI sagittal MPR reconstruction of the left mandible.

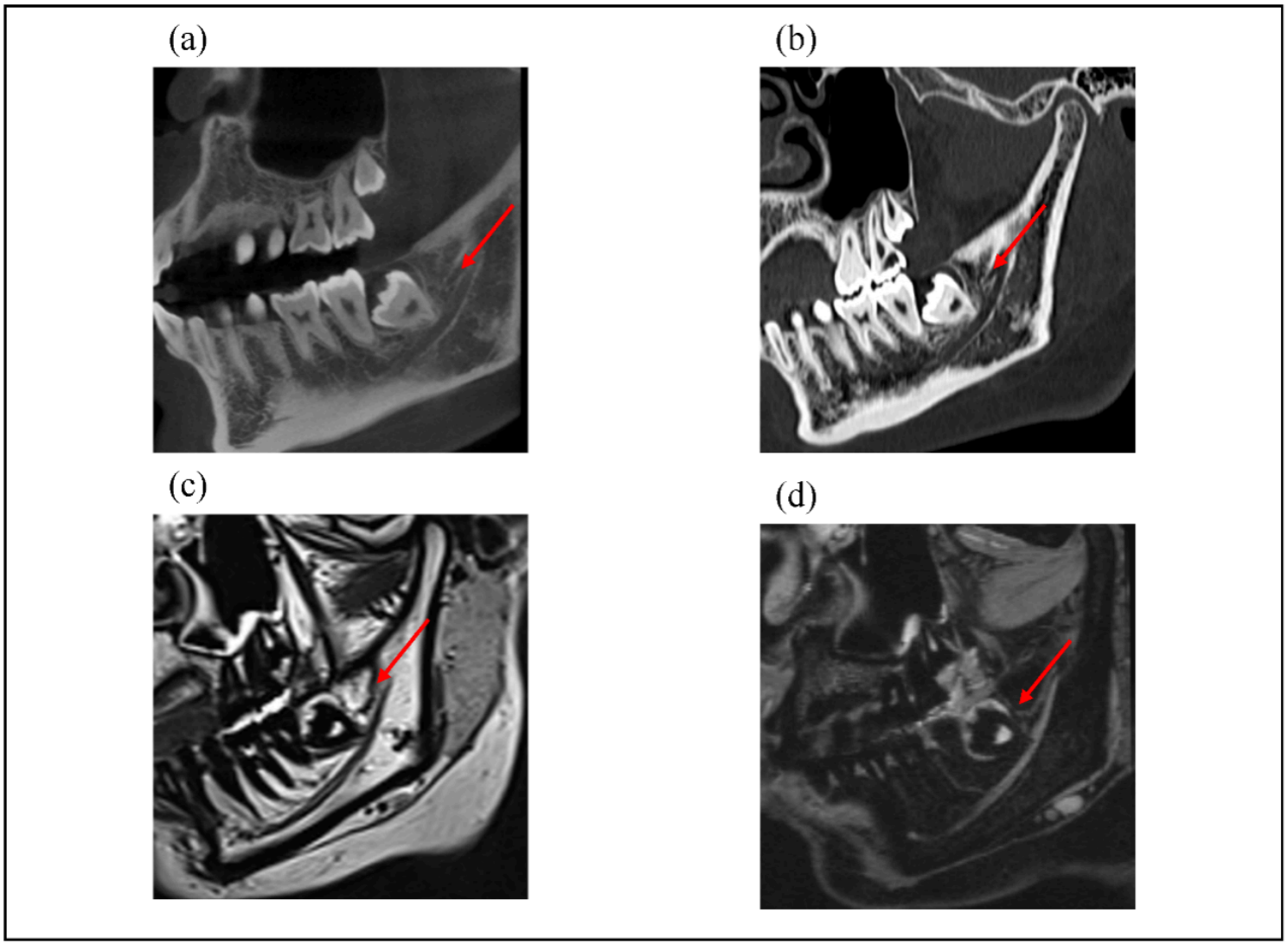


Figure 3

The manifestations of the posterior mandibular canal in the same patient under different detection methods

a The reconstructed CBCT image of the right mandibular body in sagittal view for subject 6, female, 23 years old. b Spiral CT image. c 3.0T MRI t2_tse_tra_small fov_320 sequence image. d 3.0T MRI MPR_Range sequence image

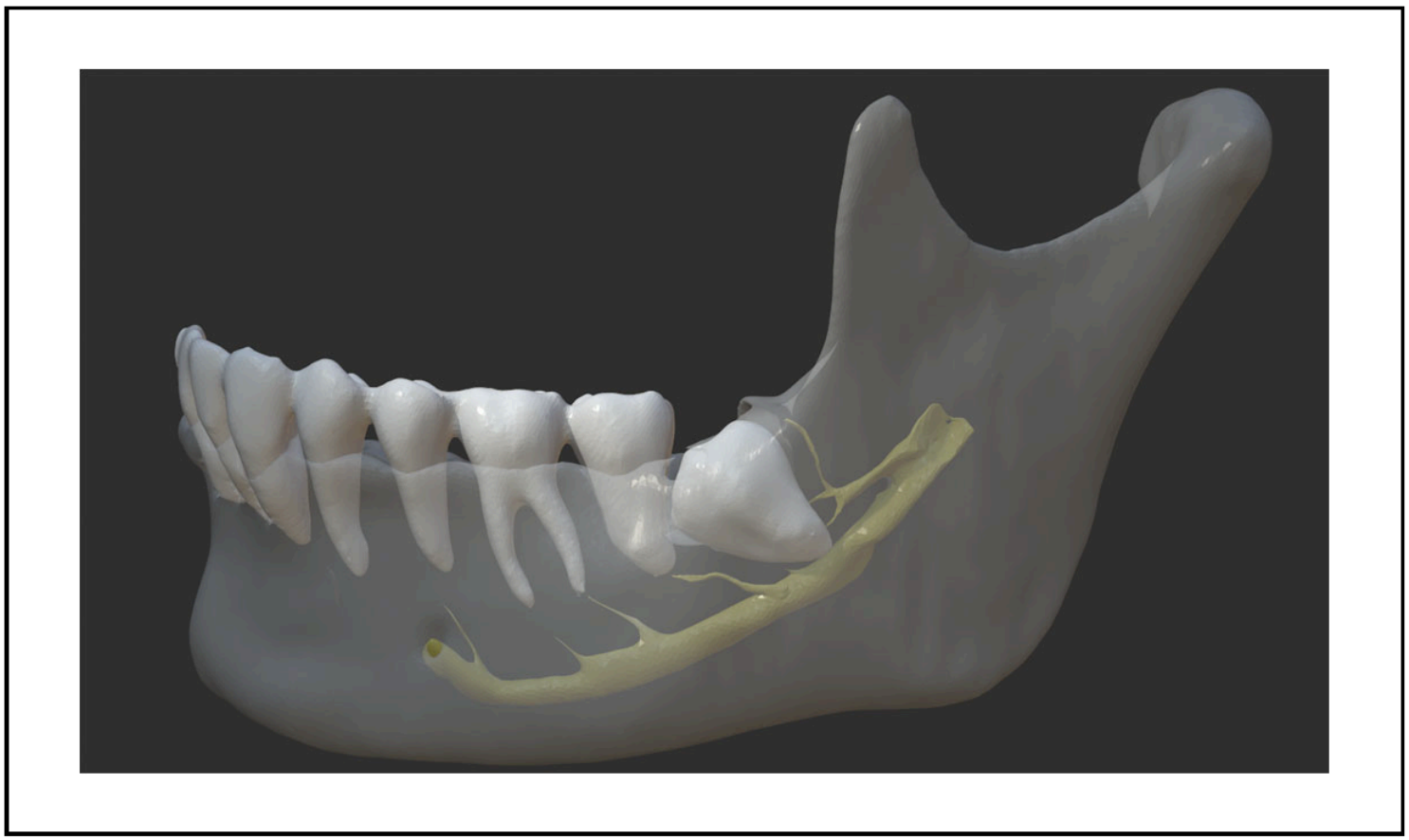


Figure 4

Three-dimensional restoration image of the posterior molar canal and its branches of the subject 6 (The mandibular teeth, mandible and posterior molar canal were marked using 3D slicer 5.10.0, and the three-dimensional morphology was reconstructed. Nomad was imported for cropping and rendering)

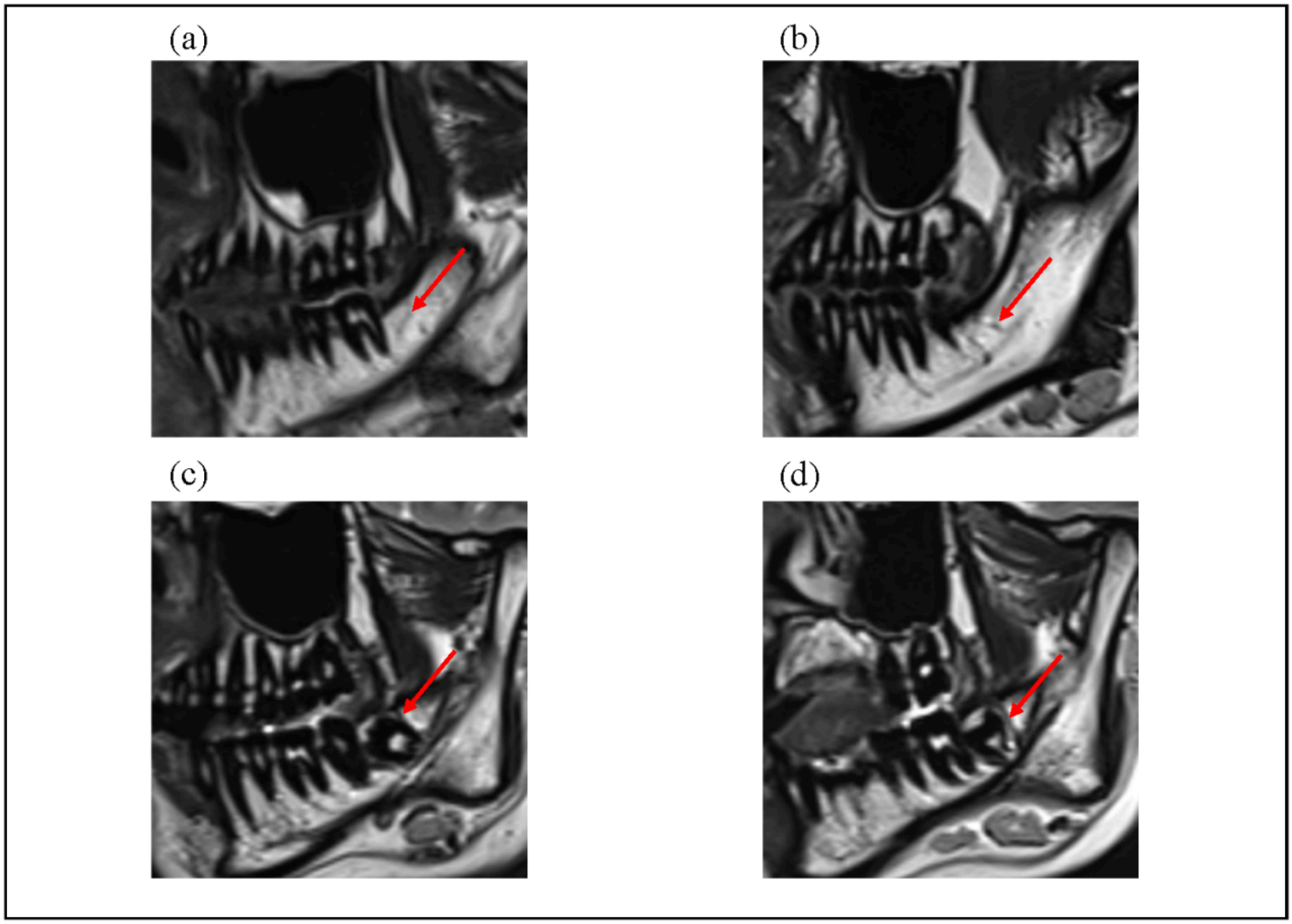


Figure 5

Two cases with special anatomical significance

a. MRI image of the right mandible of subject 6 at 3.0T. b. MRI image of the left mandible of subject 6 at 3.0T.

c MRI image of the right mandible of subject 7 at 3.0T. d MRI image of the left mandible of subject 7 at 3.0T.